

Gain-compensated metal cavity modes and a million-fold improvement of Purcell factors

Becca VanDrunen,¹ Juanjuan Ren,¹ Sebastian Franke,^{2,1} and Stephen Hughes¹

¹*Department of Physics, Engineering Physics, and Astronomy,
Queen's University, Kingston, Ontario K7L 3N6, Canada*

²*Technische Universität Berlin, Institut für Theoretische Physik,
Nichtlineare Optik und Quantenelektronik, Hardenbergstraße 36, 10623 Berlin, Germany*

Using a rigorous mode theory for gain-compensated plasmonic dimers, we demonstrate how quality factors and Purcell factors can be dramatically increased, improving the quality factors from 10 to over 26,000 and the peak Purcell factors from around 3000 to over 10 billion. Full three-dimensional calculations are presented for gold dimers in a finite-size gain medium, which allows one to easily surpass fundamental Purcell factor limits of lossy media. Within a regime of linear system response, we show how the Purcell factors are modified from the contributions from the projected local density of states as well as a non-local gain. Further, we show that the effective mode volume and radiative beta factors remain relatively constant, despite the significant enhancement of the Purcell factors.

Introduction.—Plasmonic resonators, formed by metal nanoparticles (MNPs), have become a prominent topic in nanophotonics, due in part to their unique abilities for enhancing light-matter interactions in extremely small spatial scales [1, 2]. Plasmonic resonators exploit surface plasmons, which occur at the interface of a metal and a dielectric material, and are the result of mixed electronic-optical excitations on the surface of the metal [3]. Plasmonic resonators yield electromagnetic modes that are well below the diffraction limit [1, 4], leading to improved sensing and fast generation of single photons [5, 6].

Metal based cavity modes have been explored theoretically [7, 8] and experimentally [9, 10], for a wide range of photonics applications. However, plasmonic resonators have significant decay rates, since metal is inherently a lossy material. Thus, an important goal in optical plasmonics is to find methods for alleviating this loss. Historically, optical mode theories of plasmonics were thought to be problematic [11], but this is largely caused by the use of ill-defined mode models, treating such systems like regular “normal modes”, without much consideration for losses.

Recently, accurate cavity mode theories used to describe the optical response of MNPs have been formulated, which are based on “quasinormal modes” (QNMs)—the formal solution for open cavity modes [12–15]. Similar to *normal modes*, QNMs are solutions to the source-free Helmholtz equation, but with *open* boundary conditions, where the solutions have complex eigenfrequencies and spatially diverging fields (due to temporal losses) [12, 13]. By exploiting QNM theory, it has become clear that cavity physics applies to plasmonic resonators [15, 16]. Theories based on QNMs offer a significant advantage over all-numerical approaches, which can be tedious, limited in scope, and often do not even explain the basic mechanisms of field enhancement. In contrast, a mode theory provides many physical insights, is efficient, has wide applications, and lends itself to mode quantization [17]. Moreover, the modes form a basis for computing the photonic Green function (GF), which can be used to describe a wide range of optical phenomena in both classical and quantum optics [14, 18–21].

Accounting for both material loss and radiative loss, the mode quality factor is defined from $Q = \omega_c / (2\gamma_c)$ ($2\gamma_c$ is the energy loss rate of the mode c), which for plasmonic res-

onators is much smaller than typical dielectric cavities [22]. Thus, the MNP resonances typically generate quality factors of around $Q \approx 10-20$ [23–26], which manifest in a very short cavity mode lifetime, $\tau_c = 1/\gamma_c$, e.g., a resonance of $\hbar\omega_c = 1.780 - i0.068$ eV [27], corresponds to $\tau_c \approx 0.01$ ps. Such losses prohibit many applications in coherent optics, including surface plasmon lasing and spasing [28, 29].

One potential method for mitigating this significant loss is through gain compensation, which uses material gain to suppress some of the dissipation, using linear amplification [30–32]. It is important to note that the total cavity structure must be overall lossy for the properties of cavity physics and QNM theory to apply, and also to maintain a *linear medium* response. More specifically, the entire GF is only allowed to have complex poles in the lower complex half plane. To model such a structure, both the metal and the gain are defined by a *complex* dielectric constant, where the imaginary part describes loss or gain.

Gain media has been utilized in several applications to suppress metallic losses [33–35]. For example, loss suppression in MNPs has been studied by doping them in gain [36, 37] or by adding gain to plasmonic resonators [38, 39]. While there exists some studies on how the quality factor changes as a result of gain-compensation [37, 38, 40, 41], little has been done to quantify how enhanced spontaneous emission (SE) and Purcell factors change from coupled dipole emitters. Furthermore, the concept of spasing has been an enticing area of study for decades [42–44], yet many approaches lack the robustness of a rigorous mode theory.

An important metric in nanophotonics is the Purcell factor [45], which describes the enhanced SE rate of a dipole emitter, $\Gamma(\mathbf{r}_0, \omega)$, normalized to the rate from a background homogeneous medium, $\Gamma_B(\mathbf{r}_0, \omega)$, which is $F_P \equiv \frac{3}{4\pi^2} \left(\frac{\lambda_0}{n_B} \right)^3 \frac{Q}{V_{\text{eff}}}$, where Q and V_{eff} are the mode quality factor and effective mode volume, respectively, λ_0 is the free space wavelength, and n_B is the background refractive index. This well known formula assumes the emitter is on resonance with the cavity mode and at a field maximum position, with the same polarization as the cavity mode. Traditionally, the effective mode volume describes the volume associated with mode localization, but that is no longer correct using QNMs, and the generalized mode

volume can be both complex and position dependent [46]. Moreover, when gain is added to the cavity, this formula no longer applies (even when using QNMs), and one must include a non-local correction from gain [47, 48].

In this work, we show how material gain can significantly improve the MNP cavity mode properties, using a rigorous QNM theory with linear amplification. The key findings are: (i) the effective mode volume of the mode profiles stays nearly constant as gain is introduced to the system; (ii) the Purcell factor yields a million-fold improvement when material gain is added; and (iii) the radiative beta factor also remains relatively constant. Our gain theory has a wide range of applications, including quantum sensing, as well as lasing and fundamental topics in quantum topics.

Theory.—The QNMs, $\tilde{\mathbf{f}}_\mu$, are the mode solutions to the Helmholtz equation, with open boundary conditions [14]:

$$\nabla \times \nabla \times \tilde{\mathbf{f}}_\mu(\mathbf{r}) - \left(\frac{\tilde{\omega}_\mu}{c}\right)^2 \epsilon(\mathbf{r}, \tilde{\omega}_\mu) \tilde{\mathbf{f}}_\mu(\mathbf{r}) = 0, \quad (1)$$

where c is the speed of light in a vacuum, $\tilde{\omega}_\mu$ is the QNM complex eigenfrequency $\tilde{\omega}_\mu = \omega_\mu - i\gamma_\mu$, and $\epsilon(\mathbf{r}, \tilde{\omega}_\mu)$ is the complex dielectric function. The inhomogeneous Helmholtz equation for an arbitrary polarization source can be used to define the GF, from $c^2 \nabla \times \nabla \times \mathbf{G}(\mathbf{r}, \mathbf{r}', \omega) - \omega^2 \epsilon(\mathbf{r}, \omega) \mathbf{G}(\mathbf{r}, \mathbf{r}', \omega) = \omega^2 \mathbf{1} \delta(\mathbf{r} - \mathbf{r}')$, where the electric field solution is at \mathbf{r} , when a source field dipole is at \mathbf{r}' . Within or near the cavity region, the GF can be expressed as a sum of normalized QNMs [19, 27, 49]:

$$\mathbf{G}(\mathbf{r}, \mathbf{r}_0, \omega) = \sum_\mu A_\mu(\omega) \tilde{\mathbf{f}}_\mu(\mathbf{r}) \tilde{\mathbf{f}}_\mu(\mathbf{r}_0), \quad (2)$$

where $A_\mu(\omega) = \omega/[2(\tilde{\omega}_\mu - \omega)]$ [7], and we note the vector product is unconjugated (i.e., not $\tilde{\mathbf{f}}_\mu \tilde{\mathbf{f}}_\mu^*$), which is a consequence of using a non-Hermitian theory. When a single QNM dominates, $\mu = c$, then the GF is simply

$$\mathbf{G}_c(\mathbf{r}, \mathbf{r}_0, \omega) \approx A_c(\omega) \tilde{\mathbf{f}}_c(\mathbf{r}) \tilde{\mathbf{f}}_c(\mathbf{r}_0). \quad (3)$$

In a lossy material system with no gain, the SE rate for a dipole emitter at a location \mathbf{r}_0 is determined from the (projected) local density of states (LDOS) [12, 27]:

$$\Gamma_{\text{LDOS}}^{\text{SE}}(\mathbf{r}_0, \omega) = \frac{2}{\hbar \epsilon_0} \mathbf{d} \cdot \text{Im}[\mathbf{G}(\mathbf{r}_0, \mathbf{r}_0, \omega)] \cdot \mathbf{d}, \quad (4)$$

and using a single QNM expansion approximation, \mathbf{G} becomes \mathbf{G}_c , as shown in Eq. (3). The SE rate for a dipole in a homogeneous medium, $\Gamma_{\text{B}}(\mathbf{r}_0, \omega)$, is similarly obtained by replacing \mathbf{G} by \mathbf{G}_{B} (the GF of a homogeneous medium), which is known analytically. The LDOS Purcell factor is then given by [12, 27, 50]

$$F_{\text{P}}^{\text{LDOS}}(\mathbf{r}_0, \omega) = 1 + \frac{6\pi c^3}{\omega^3 \eta_{\text{B}}} \mathbf{n}_{\text{d}} \cdot \text{Im}[\mathbf{G}(\mathbf{r}_0, \mathbf{r}_0, \omega)] \cdot \mathbf{n}_{\text{d}}, \quad (5)$$

and $F_{\text{P}}^{\text{QNM,LDOS}}$ is obtained by using $\mathbf{G} \rightarrow \mathbf{G}_c$.

However, this classical LDOS formalism for the Purcell factor is not correct in the presence of a linear gain medium.

Instead, the total SE rate can be written as [47, 48]

$$\Gamma_{\text{tot}}^{\text{SE}}(\mathbf{r}_0, \omega) = \Gamma_{\text{LDOS}}^{\text{SE}}(\mathbf{r}_0, \omega) + \Gamma_{\text{gain}}^{\text{SE}}(\mathbf{r}_0, \omega), \quad (6)$$

which notably contains an extra net-positive term related to gain region added to the traditional LDOS term; this correction can be derived quantum mechanically [14, 47] or classically [48]. The total Purcell factor is then

$$F_{\text{P}}(\mathbf{r}_0, \omega) = 1 + \frac{\Gamma_{\text{tot}}^{\text{SE}}(\mathbf{r}_0, \omega)}{\Gamma_{\text{B}}(\mathbf{r}_0, \omega)}. \quad (7)$$

In origin, the well known LDOS-SE formula is linked to the GF identity, $\int_{\mathbb{R}^3} d\mathbf{s} \epsilon_I(\mathbf{s}) \mathbf{G}(\mathbf{r}, \mathbf{s}) \cdot \mathbf{G}^*(\mathbf{s}, \mathbf{r}') = \text{Im}[\mathbf{G}(\mathbf{r}, \mathbf{r}')]$, which involves an integration over all space. However, from this identity, one must subtract the contribution from the gain, and this results in *adding* the separate gain contribution term, which is given by [47]

$$\Gamma_{\text{gain}}^{\text{SE}}(\mathbf{r}_0, \omega) = \frac{2}{\hbar \epsilon_0} \mathbf{d} \cdot \mathbf{K}(\mathbf{r}_0, \mathbf{r}_0, \omega) \cdot \mathbf{d}, \quad (8)$$

where

$$\mathbf{K}(\mathbf{r}_0, \mathbf{r}_0, \omega) = \int_{V_{\text{gain}}} d\mathbf{s} |\text{Im}[\epsilon^{\text{gain}}(\mathbf{s})]| \mathbf{G}(\mathbf{r}_0, \mathbf{s}, \omega) \cdot \mathbf{G}^*(\mathbf{s}, \mathbf{r}_0, \omega). \quad (9)$$

In the case of a single dominant QNM, $\mu = c$, then

$$\Gamma_{\text{gain}}^{\text{SE}}(\mathbf{r}_0, \omega) = \frac{2|\mathbf{d}|^2}{\hbar \epsilon_0} |A_c(\omega)|^2 |\mathbf{n}_{\text{d}} \cdot \tilde{\mathbf{f}}_c(\mathbf{r}_0)|^2 \times \int_{V_{\text{gain}}} d\mathbf{s} |\text{Im}[\epsilon^{\text{gain}}(\mathbf{s})]| |\tilde{\mathbf{f}}_c(\mathbf{s})|^2. \quad (10)$$

From the perspective of classical power flow arguments [48], the total Purcell factor can be written as

$$F_{\text{P}}(\mathbf{r}_0, \omega) = \frac{P_{\text{LDOS}}(\mathbf{r}_0, \omega) + P_{\text{gain}}(\mathbf{r}_0, \omega)}{P_0(\omega)}, \quad (11)$$

where P_{LDOS} and P_0 are the power flow from the point dipole with and without the cavity structure (background medium), respectively, and P_{gain} is the power flowing out from the gain region (net-positive). Equation (11) can be solved using QNMs or numerically. The total Purcell factors can also be written as $F_{\text{P}}(\mathbf{r}_0, \omega) = \frac{P_{\text{far}}(\mathbf{r}_0, \omega) + P_{\text{loss}}(\mathbf{r}_0, \omega)}{P_0(\omega)}$, where P_{far} and P_{loss} are power radiated to far field region and dissipated within lossy region, respectively.

From this general SE decay theory, one can also determine the radiative beta factor (β -factor), which represents the probability that an emitted photon will decay radiatively to the far field [27]. Generally, there are both radiative and non-radiative β -factors, and the sum of these must equal one [8]. The radiative beta factor is [48]

$$\beta^{\text{rad}}(\mathbf{r}_0, \omega) = \frac{P_{\text{far}}(\mathbf{r}_0, \omega)}{P_{\text{far}}(\mathbf{r}_0, \omega) + P_{\text{loss}}(\mathbf{r}_0, \omega)}, \quad (12)$$

which can also be written equivalently in terms of P_{LDOS} and P_{gain} based on the power conservation law [48].

Results.—The main MNP cavity structure we model con-

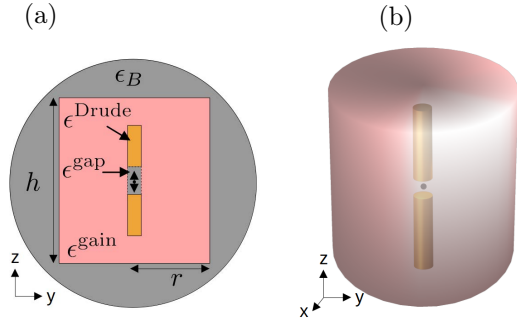


Figure 1 : (a) A 2D view of the resonator system. The dielectric functions for each material are labeled, where the background medium has $\epsilon_B = 2.25$ ($\epsilon_B = n_B^2$), the gain region has $\epsilon^{\text{gain}} = 2.25 - i\alpha_g$ (where α_g is the gain parameter), the gold nanorods have ϵ^{Drude} which is governed by the Drude model (see text), and the gap region has $\epsilon^{\text{gap}} = 2.25$. The gold nanorods have a length of 80 nm, a radius of 10 nm, and the gap distance is 20 nm; h represents the height of the gain region, and is 400 nm, and r represents the radius of the gain region, which is 200 nm. (b) 3D version of the system (as used in our model).

sists of a gold dimer enclosed in a finite-sized cylindrical region of gain, as shown in Fig. 1. The dielectric constant for the gold is described by the Drude model, $\epsilon^{\text{Drude}}(\omega) = 1 - \frac{\omega_p^2}{\omega^2 + i\omega\gamma_p}$, with $\hbar\omega_p = 8.2934$ eV and $\hbar\gamma_p = 0.0928$ eV. The gap region between the nanorods (where the dipole sits) is considered to have a real permittivity. The gain region has a permittivity of $\epsilon^{\text{gain}} = 2.25 - i\alpha_g$, so the gap region simply takes the real component of this. A real example of a gain material is Rh6G dye in PMMA, e.g., with permittivity of $\epsilon^{\text{gain}} = 2.25 - i0.006$ [31, 51]. Gallium Arsenide quantum wells can also have rather large gain values, e.g., $\epsilon^{\text{gain}} = 11.76 - i0.208$ [31, 52]. We assume the gain is dispersionless, but gain dispersion results are discussed in the Supplementary Material (SM) [53], and do not affect our general findings. For all calculations below, we obtain the QNMs numerically using a complex frequency approach, implemented in COMSOL [7, 27].

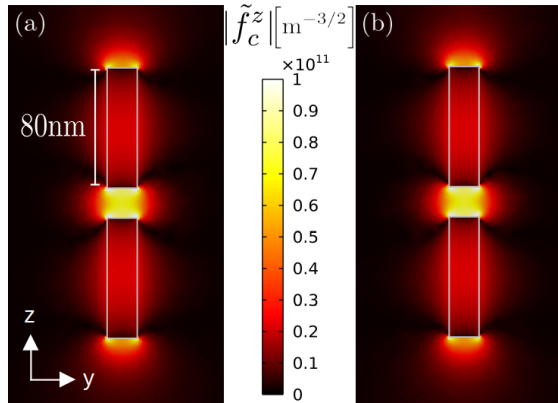


Figure 2 : Surface plots of the computed QNM profile (using the dominant field component) for the plasmonic resonator system (a) without gain, and (b) with gain, using $\alpha_g = 2.54 \cdot 10^{-1}$.

The vector-field QNM is dominated by z -polarization, that peaks in frequency near $\hbar\omega \approx 1.2$ eV. As can be seen

in Fig. 2, the spatial profile of the QNM is similar with and without the gain medium. Furthermore, this can be verified quantitatively, by calculating the effective mode volume, $V_{\text{eff}}^{-1}(\mathbf{r}_0) = \epsilon(\mathbf{r}_0)\text{Re}[\tilde{f}_c^2(\mathbf{r}_0)]$ from QNM theory. See SM [53] for the computed effective mode volume at gap center. In stark contrast to lasing modes, and constant-flux modes, which can observe drastic changes to the spatial modes, the linear-gain-assisted modes remain relatively similar [54, 55].

For the two cases shown in Fig. 2, the complex QNM eigenfrequencies are $\hbar\tilde{\omega}_c = 1.198 - i5.934 \cdot 10^{-2}$ eV and $\hbar\tilde{\omega}_c = 1.195 - i2.238 \cdot 10^{-5}$ eV, respectively. This leads to QNM quality factors Q of 10 and 26,698, respectively, showing that a significant improvement in Q is possible.

In the presence of gain, the LDOS Purcell factor of a dipole placed at the dimer gap center can be calculated using Eq. (5) and checked against a full numerical dipole calculation [27, 48]. The LDOS Purcell factor gives insights into how the gain medium impacts the SE rates.

A summary of the Purcell factors with and without gain is shown in Fig. 3. Fig. 3a shows the LDOS Purcell factors for α_g from 0 to $2.2 \cdot 10^{-1}$; the agreement between the QNM method (curves) and the full dipole method (symbols) is excellent, and we stress there are no fitting parameters used in this model. A summary of the Purcell factor at a fixed frequency over a range of spatial points within the gap center can be found in the SM [53]. This exhibits the power of our QNM theory and also shows that significant Purcell factors occur over a large spatial domain.

Moreover, both Figs. 3a and 3b (which increases the gain to $\alpha_g = 2.5 \cdot 10^{-1} \sim 2.54 \cdot 10^{-1}$) demonstrate a substantial increase in the LDOS Purcell factor. Specifically, the LDOS Purcell factor experiences an increase by a factor of nearly 3000, between the LDOS Purcell factors for $\alpha_g = 0$ and $\alpha_g = 2.54 \cdot 10^{-1}$. Since V_{eff} is similar with and without gain, this increase is primarily caused by *gain compensating* the loss. As anticipated, there are values of the LDOS Purcell factor that are negative for certain frequency values (as the LDOS becomes negative). We note again that there is nothing unphysical about a negative LDOS; it means that there is more local power flow back to the dipole location than out of the dipole, but the entire cavity system is still net lossy. The sign of the LDOS Purcell factor is dependent on position, and does not relate to other quantities such as the quality factor [47]. Negative LDOS Purcell factors have no implications on linear amplification either.

Next, we show the total Purcell factor in Fig. 3c, corresponding to the α_g values from Fig. 3b. There are no longer any negative values for the total Purcell factor, and the (correct) enhanced SE has been further increased, by many orders of magnitude, peaking at a value of $2.08 \cdot 10^{10}$ when the gain value is $2.54 \cdot 10^{-1}$, yielding an increase by a factor of $7.1 \cdot 10^6$ from the case with no gain. As anticipated by our analytical QNM theory, the lineshapes also deviate significantly from Lorentzian and become similar to Lorentzian-squared when the gain contribution dominates, sharing some features and applications of resonances near exceptional points [14, 56, 57], such as enhanced sensing.

As mentioned before, it is crucial for the region of *linear amplification* that we ensure the QNM peak eigenfrequency

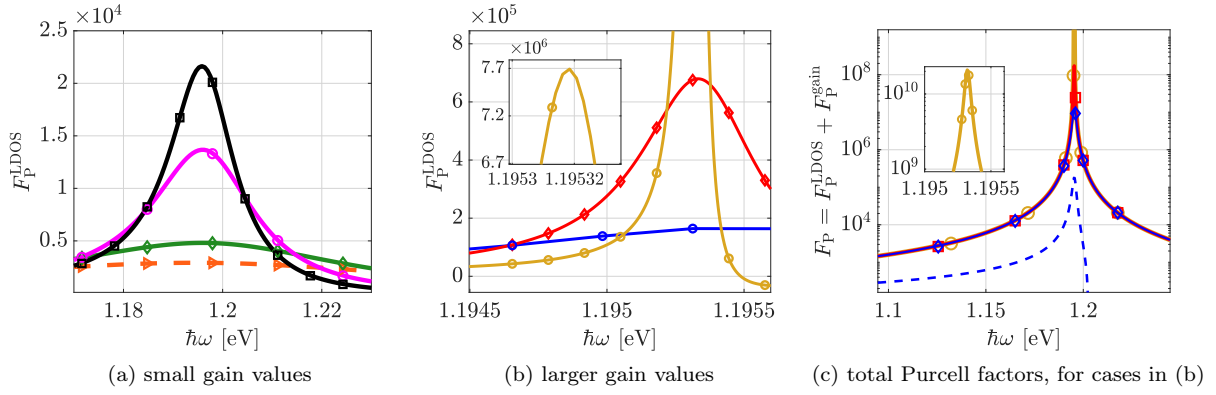


Figure 3 : (a) LDOS Purcell factors for various α_g , corresponding to the model in Fig. 1. The curves show the QNM method, calculated with Eq. (5), and the symbols show the full dipole numerical solution with Eq. (11). The orange dashed line/symbols are for the case with $\alpha_g = 0$, the green line/points represent $\alpha_g = 1 \cdot 10^{-1}$, the magenta line/points represent $\alpha_g = 2 \cdot 10^{-1}$, and the black line/points represent $\alpha_g = 2.2 \cdot 10^{-1}$. The γ_c values for each curve in increasing order of α_g are: γ_0 , $0.61\gamma_0$, $0.21\gamma_0$, $0.13\gamma_0$, where $\gamma_0 = 9.016 \cdot 10^{13}$ rads/s. (b) LDOS Purcell factors for larger values of α_g . The blue line/points represent the case where $\alpha_g = 2.5 \cdot 10^{-1}$, the red line/points represents the case where $\alpha_g = 2.53 \cdot 10^{-1}$, and the gold line/points represents the case where $\alpha_g = 2.54 \cdot 10^{-1}$. The γ_c values for each curve in increasing order of α_g are: $0.02\gamma_0$, $0.004\gamma_0$, and $0.0004\gamma_0$. The bandwidth ($2\gamma_c$) for each curve in increasing order of α_g are: 2.4 meV, 0.48 meV, and 0.048 meV. (c) Total Purcell factor over a range of energies for three different values of α_g , calculated with Eq. (7) for the QNM method, and a full numerical dipole method to confirm the results, using Eq. (11). The blue, red, and gold line/points correspond to the same α_g values used in Fig. 3b, all plotted on a logarithmic y -axis. The dashed blue line represents the LDOS Purcell factor when $\alpha_g = 2.5 \cdot 10^{-1}$, which shows a significant difference (and becomes negative at larger frequencies). The bandwidths in increasing order of α_g are: 2.4 meV, 0.48 meV, and 0.048 meV.

$\tilde{\omega}_c = \omega_c - i\gamma_c$ has a positive value for γ_c . This threshold has been found heuristically [37], however the QNM method provides a more rigorous definition of the linear amplification regime through the resonant eigenfrequency.

It is important to note that the gain contribution to enhancing the LDOS Purcell factor (with gain) does not really affect the bandwidth, and is precisely $2\gamma_c$ with a lineshape of a Lorentzian squared function [see Eq. (10)]. This is quite different to lossy media and dielectric cavities, where the Purcell factors are often maximized to near 1000, and the Q factors to around 1 million (for example, see Refs. [58–60]), and the bandwidths are much narrower, since these are inversely proportional to Q . The narrow bandwidths in high Q dielectric cavities are also influenced from manufacturing disorder, so further improvements, even with complex design, are not so beneficial. As a state-of-the-art example with sub-wavelength mode volumes, impressive topologically-optimized dielectric cavities can yield a peak Purcell factor on the order of $F_P = 6 \times 10^3$ [61], with a measured value of roughly $F_P = 1 \times 10^3$, due to manufacturing imperfections and disorder.

We note that for our peak Purcell values exceeding 10 billion, the bandwidth is around 0.048 meV, while a 1 million quality-factor dielectric design working at 200 THz (1.5 microns) has a much smaller bandwidth of 0.00074 meV.

Finally, we examine the modified beta factors, using Eq. (12). In the linear regime, the β -factor must have an upper limit of 1, which is the β -factor for an ideal lossless dielectric system, and values surpassing this limit are indicative of the lasing regime [62]. With no gain, the beta factor from the metal dimer cavity (on resonance) is 0.33, and when $\alpha_g = 0.254$, the beta factor is 0.376. Further insights about the beta factor can be found in the SM [53]. Having

a large radiative beta factor is useful for many applications, such as lasing/spasing and sensing applications. [63–66].

In summary, using a rigorous and powerful QNM theory, the enhanced SE rates of a dipole emitter in a plasmonic resonator system were studied, with and without gain. Using material gain to compensate for the lossy nature of the gold dimer, the LDOS and total Purcell factors were shown to be substantially increased; the Purcell factor with no gain peaks around 2900, but with a maximum gain value of $\alpha_g = 2.54 \cdot 10^{-1}$ (for linear amplification) the LDOS and total Purcell factors peak at $7.7 \cdot 10^6$ and $2.08 \cdot 10^{10}$, respectively. We also discussed how we ensure a regime of linear amplification, and demonstrated that a single QNM theory worked quantitatively well by comparing with numerically exact simulations (subject to numerical limitations). Determining how gain-compensation of loss impacts properties, such as the enhanced SE, is important for developing accurate models of plasmonic lasers, quantum sensors, and lossy cavity systems that can possibly achieve the regime of ultrastrong light-matter coupling ($g/\omega_c > 0.1$ [67–69], where g is the cavity-dipole coupling rate).

We acknowledge funding from Queen’s University, Canada, the Canadian Foundation for Innovation (CFI), the Natural Sciences and Engineering Research Council of Canada (NSERC), and CMC Microsystems for the provision of COMSOL Multiphysics. We also acknowledge support from the Alexander von Humboldt Foundation through a Humboldt Research Award.

Disclosures.—The authors declare no conflicts of interest.

Data Availability.—Data underlying the results in this paper are not publicly available at this time but may be obtained from the authors upon reasonable request.

-
- [1] M. R. Gonçalves, H. Minassian, and A. Melikyan, Plasmonic resonators: fundamental properties and applications, *Journal of Physics D: Applied Physics* **53**, 443002 (2020).
- [2] A. Krasnok and A. Alù, Active nanophotonics, *Proceedings of the IEEE* **108**, 628 (2020).
- [3] J. M. Pitarke, V. M. Silkin, E. V. Chulkov, and P. M. Echenique, Theory of surface plasmons and surface-plasmon polaritons, *Reports on Progress in Physics* **70**, 1 (2006).
- [4] T.-B. Wang, X.-W. Wen, C.-P. Yin, and H.-Z. Wang, The transmission characteristics of surface plasmon polaritons in ring resonator, *Opt. Express* **17**, 24096 (2009).
- [5] Y.-F. Xiao, B.-B. Li, X. Jiang, X. Hu, Y. Li, and Q. Gong, High quality factor, small mode volume, ring-type plasmonic microresonator on a silver chip, *Journal of Physics B: Atomic, Molecular and Optical Physics* **43**, 035402 (2010).
- [6] A. Østerkryger, *Engineering of nanophotonic structures for quantum information applications.*, Ph.D. thesis (2018).
- [7] Q. Bai, M. Perrin, C. Sauvan, J.-P. Hugonin, and P. Lalanne, Efficient and intuitive method for the analysis of light scattering by a resonant nanostructure, *Opt. Express* **21**, 27371 (2013).
- [8] S. Hughes, S. Franke, C. Gustin, M. Kamandar Dezfouli, A. Knorr, and M. Richter, Theory and limits of on-demand single-photon sources using plasmonic resonators: A quantized quasinormal mode approach, *ACS Photonics* **6**, 2168 (2019).
- [9] J. Chae, B. Lahiri, and A. Centrone, Engineering near-field seira enhancements in plasmonic resonators, *ACS Photonics* **3**, 87 (2016).
- [10] R. Chikkaraddy, B. de Nijs, F. Benz, S. J. Barrow, O. A. Scherman, E. Rosta, A. Demetriadou, P. Fox, O. Hess, and J. J. Baumberg, Single-molecule strong coupling at room temperature in plasmonic nanocavities, *Nature* **535**, 127 (2016).
- [11] A. F. Koenderink, On the use of purcell factors for plasmon antennas, *Optics Letters* **35**, 4208 (2010).
- [12] P. T. Kristensen and S. Hughes, Modes and Mode Volumes of Leaky Optical Cavities and Plasmonic Nanoresonators, *ACS Photonics* **1**, 2 (2014).
- [13] P. T. Kristensen, K. Herrmann, F. Intravaia, and K. Busch, Modeling electromagnetic resonators using quasinormal modes, *Adv. Opt. Photonics* **12**, 612 (2020).
- [14] J. Ren, S. Franke, and S. Hughes, Quasinormal modes, local density of states, and Classical Purcell factors for coupled loss-gain resonators, *Phys. Rev. X* **11**, 041020 (2021).
- [15] P. Lalanne, W. Yan, K. Vynck, C. Sauvan, and J.-P. Hugonin, Light interaction with photonic and plasmonic resonances, *Laser Photonics Rev.* **12**, 1700113 (2018).
- [16] M. Perrin, J. Yang, and P. Lalanne, Analytical treatment of the interaction between light, plasmonic and quantum resonances: quasi-normal mode expansion, in *Quantum Sensing and Nano Electronics and Photonics XIII*, Vol. 9755, edited by M. Razeghi, International Society for Optics and Photonics (SPIE, 2016) p. 97551J.
- [17] S. Franke, S. Hughes, M. K. Dezfouli, P. T. Kristensen, K. Busch, A. Knorr, and M. Richter, Quantization of quasinormal modes for open cavities and plasmonic cavity quantum electrodynamics, *Phys. Rev. Lett.* **122**, 213901 (2019).
- [18] C. P. Van Vlack, *Dyadic Green functions and their applications in classical and quantum nanophotonics*, PhD Thesis, Queen's University (2012).
- [19] R.-C. Ge, P. T. Kristensen, J. F. Young, and S. Hughes, Quasinormal mode approach to modelling light-emission and propagation in nanoplasmonics, *New J. Phys.* **16**, 113048 (2014).
- [20] H. T. Dung, L. Knöll, and D.-G. Welsch, Three-dimensional quantization of the electromagnetic field in dispersive and absorbing inhomogeneous dielectrics, *Phys. Rev. A* **57**, 3931 (1998).
- [21] M. Righini, A. Zelenina, and C. e. a. Girard, Parallel and selective trapping in a patterned plasmonic landscape, *Nature Physics* **3**, 477–480 (2007).
- [22] A. Sharma and S. C. Shrivastava, Analysis of resonant frequency and quality factor of dielectric resonator at different dielectric constant materials, in *2008 International Conference on Recent Advances in Microwave Theory and Applications* (2008) pp. 593–595.
- [23] K. G. Cognée, H. M. Doeleman, P. Lalanne, and A. F. Koenderink, Cooperative interactions between nano-antennas in a high-Q cavity for unidirectional light sources, *Light: Sci. Appl.* **8**, 115 (2019).
- [24] M. Melli, A. Polyakov, D. Gargas, C. Huynh, L. Scipioni, W. Bao, D. F. Ogletree, P. J. Schuck, S. Cabrini, and A. Weber-Bargioni, Reaching the theoretical resonance quality factor limit in coaxial plasmonic nanoresonators fabricated by helium ion lithography, *Nano Letters* **13**, 2687 (2013).
- [25] G. Lilley, M. Messner, and K. Unterrainer, Improving the quality factor of the localized surface plasmon resonance, *Opt. Mater. Express* **5**, 2112 (2015).
- [26] M. Kuttge, F. J. García de Abajo, and A. Polman, Ultra-small mode volume plasmonic nanodisk resonators, *Nano Letters* **10**, 1537 (2010), pMID: 19813755.
- [27] J. Ren, S. Franke, A. Knorr, M. Richter, and S. Hughes, Near-field to far-field transformations of optical quasinormal modes and efficient calculation of quantized quasinormal modes for open cavities and plasmonic resonators, *Phys. Rev. B* **101**, 205402 (2020).
- [28] M. I. Stockman, Spasers explained, *Nature Photonics* **2**, 327 (2008).
- [29] M. I. Stockman, Spaser action, loss compensation, and stability in plasmonic systems with gain, *Physical Review Letters* **106**, 156802 (2011).
- [30] M. I. Stockman, Loss compensation by gain and spasing, *Philosophical Transactions of the Royal Society A: Mathematical, Physical and Engineering Sciences* **369**, 3510 (2011).
- [31] S. C. Russev, G. G. Tsutsumanova, and A. N. Tzonev, Conditions for loss compensation of surface plasmon polaritons propagation on a metal/gain medium boundary, *Plasmonics* **7**, 151 (2012).
- [32] A. Veltri and A. Aradian, Optical response of a metallic nanoparticle immersed in a medium with optical gain, *Phys. Rev. B* **85**, 115429 (2012).
- [33] I. De Leon and P. Berini, Amplification of long-range surface plasmons by a dipolar gain medium, *Nature Photonics* **4**, 382–387 (2010).
- [34] M. A. Noginov, Compensation of surface plasmon loss by gain in dielectric medium, *Journal of Nanophotonics* **2**, 021855 (2008).
- [35] P. Berini and I. De Leon, Surface plasmon–polariton amplifiers and lasers, *Nature Photonics* **6**, 16–24 (2011).
- [36] V. Pustovit, F. Capolino, and A. Aradian, Cooperative plasmon-mediated effects and loss compensation by gain dyes near a metal nanoparticle, *J. Opt. Soc. Am. B* **32**, 188 (2015).
- [37] S.-Y. Liu, J. Li, F. Zhou, L. Gan, and Z.-Y. Li, Efficient surface plasmon amplification from gain-assisted gold nanorods, *Optics Letters* **36**, 1296 (2011).
- [38] J. Cai, Y. J. Zhou, Y. Zhang, and Q. Y. Li, Gain-assisted

- ultra-high-q spoof plasmonic resonator for the sensing of polar liquids, *Opt. Express* **26**, 25460 (2018).
- [39] A. Fang, Z. Huang, T. Koschny, and C. M. Soukoulis, Overcoming the losses of a split ring resonator array with gain, *Opt. Express* **19**, 12688 (2011).
- [40] P. Ding, J. He, J. Wang, C. Fan, G. Cai, and E. Liang, Low-threshold surface plasmon amplification from a gain-assisted core-shell nanoparticle with broken symmetry, *Journal of Optics* **15**, 105001 (2013).
- [41] Z. Wang, X. Meng, A. V. Kildishev, A. Boltasseva, and V. M. Shalaev, Nanolasers enabled by metallic nanoparticles: From spasers to random lasers, *Laser & Photonics Reviews* **11**, 1700212 (2017).
- [42] X.-L. Zhong and Z.-Y. Li, All-analytical semiclassical theory of spaser performance in a plasmonic nanocavity, *Phys. Rev. B* **88**, 085101 (2013).
- [43] X. L. Zhong, M. H. Hong, and Z. Y. Li, Spaser in plasmonic nano-antenna evaluated by an analytical theory, *Applied Physics A* **115**, 5–11 (2013).
- [44] T. Warnakula, M. I. Stockman, and M. Premaratne, Improved scheme for modeling a spaser made of identical gain elements, *J. Opt. Soc. Am. B* **35**, 1397 (2018).
- [45] S. V. Gaponenko, *Introduction to Nanophotonics* (Cambridge University Press, 2010).
- [46] P. T. Kristensen, J. R. de Lasson, and N. Gregersen, Calculation, normalization, and perturbation of quasinormal modes in coupled cavity-waveguide systems, *Opt. Lett.* **39**, 6359 (2014).
- [47] S. Franke, J. Ren, M. Richter, A. Knorr, and S. Hughes, Fermi's golden rule for spontaneous emission in absorptive and amplifying media, *Phys. Rev. Lett.* **127**, 013602 (2021).
- [48] J. Ren, S. Franke, B. VanDrunen, and S. Hughes, *Classical Purcell factors and spontaneous emission decay rates in a linear gain medium* (2023), arXiv:2305.12049 [physics, physics:quant-ph].
- [49] P. T. Leung, S. Y. Liu, and K. Young, Completeness and orthogonality of quasinormal modes in leaky optical cavities, *Phys. Rev. A* **49**, 3057 (1994).
- [50] P. Anger, P. Bharadwaj, and L. Novotny, Enhancement and quenching of single-molecule fluorescence, *Phys. Rev. Lett.* **96**, 113002 (2006).
- [51] M. A. Noginov, V. A. Podolskiy, G. Zhu, M. Mayy, M. Bahoura, J. A. Adegoke, B. A. Ritzo, and K. Reynolds, Compensation of loss in propagating surface plasmon polariton by gain in adjacent dielectric medium, *Opt. Express* **16**, 1385 (2008).
- [52] S. W. Corzine, R.-H. Yan, and L. A. Coldren, in *Quantum Well Lasers*, edited by P. S. Zory (Academic Press, San Diego, 1993).
- [53] See supplemental material at [url will be inserted by publisher] for further information on the effective mode volume, calculations in a dispersive gain media, and the radiative beta factor.
- [54] L. Ge, Y. D. Chong, S. Rotter, H. E. Türeci, and A. D. Stone, Unconventional modes in lasers with spatially varying gain and loss, *Phys. Rev. A* **84**, 023820 (2011).
- [55] I. V. Doronin, E. S. Andrianov, and A. A. Zyablovsky, Overcoming the diffraction limit on the size of dielectric resonators using an amplifying medium, *Phys. Rev. Lett.* **129**, 133901 (2022).
- [56] A. Pick, B. Zhen, O. D. Miller, C. W. Hsu, F. Hernandez, A. W. Rodriguez, M. Soljačić, and S. G. Johnson, General theory of spontaneous emission near exceptional points, *Opt. Express* **25**, 12325 (2017).
- [57] M.-A. Miri and A. Alù, Exceptional points in optics and photonics, *Science* **363**, eaar7709 (2019).
- [58] M. Minkov, V. Savona, and D. Gerace, Photonic crystal slab cavity simultaneously optimized for ultra-high Q/V and vertical radiation coupling, *Applied Physics Letters* **111**, 131104 (2017).
- [59] J. Vasco and V. Savona, Global optimization of an encapsulated si/sio₂ l3 cavity with a 43 million quality factor, *Scientific Reports* **11**, 10121 (2021).
- [60] N. Granchi, F. Intonti, M. Florescu, P. D. García, M. Gurioli, and G. Arregui, Q-factor optimization of modes in ordered and disordered photonic systems using non-hermitian perturbation theory, *ACS photonics* **10**, 2808 (2023).
- [61] M. Albrechtsen, B. Vosoughi Lahijani, R. E. Christiansen, V. T. H. Nguyen, L. N. Casses, S. E. Hansen, N. Stenger, O. Sigmund, H. Jansen, J. Mørk, *et al.*, Nanometer-scale photon confinement in topology-optimized dielectric cavities, *Nature Communications* **13**, 6281 (2022).
- [62] C. Carlson and S. Hughes, Dissipative modes, Purcell factors, and directional beta factors in gold bowtie nanoantenna structures, *Phys. Rev. B* **102**, 155301 (2020).
- [63] G. Kewes, K. Herrmann, R. Rodríguez-Oliveros, A. Kuhllicke, O. Benson, and K. Busch, Limitations of particle-based spasers, *Phys. Rev. Lett.* **118**, 237402 (2017).
- [64] T. Mikhailova, A. Shaposhnikov, S. Tomilin, and D. Alentiev, Nanostructures with magneto-optical and plasmonic response for optical sensors and nanophotonic devices, in *Journal of Physics: Conference Series*, Vol. 1410 (IOP Publishing, 2019) p. 012163.
- [65] Y. Gao, H. Wu, N. Zhou, Y. Yang, X. Guo, P. Wang, J. You, Y. Gu, G. Lu, Q. Gong, and L. Tong, Single-nanorod plasmon nanolaser: A route toward a three-dimensional ultra-confined lasing mode, *Phys. Rev. A* **102**, 063520 (2020).
- [66] K. Caicedo, A. Cathey, M. Infusino, A. Aradian, and A. Veltri, Gain-driven singular resonances in active core-shell and nano-shell plasmonic particles, *J. Opt. Soc. Am. B* **39**, 107 (2022).
- [67] A. F. Kockum, A. Miranowicz, S. D. Liberato, S. Savasta, and F. Nori, Ultrastrong coupling between light and matter, *Nature Reviews Physics* **1**, 19 (2019).
- [68] P. Forn-Díaz, L. Lamata, E. Rico, J. Kono, and E. Solano, Ultrastrong coupling regimes of light-matter interaction, *Rev. Mod. Phys.* **91**, 025005 (2019).
- [69] W. Salmon, C. Gustin, A. Settineri, O. D. Stefano, D. Zueco, S. Savasta, F. Nori, and S. Hughes, Gauge-independent emission spectra and quantum correlations in the ultrastrong coupling regime of open system cavity-QED, *Nanophotonics* **11**, 1573 (2022).